

# Heat Storage in Eutectic Alloys

C. ERNEST BIRCHENALL AND ALAN F. RIECHMAN

Classical thermodynamic equations based on the regular solution approximation yield enthalpic changes for eutectic transformation that agree roughly with values measured for several binary and ternary alloy systems by differential scanning calorimetry or differential thermal analysis. Restricting measurements to binary and ternary alloys of the relatively plentiful elements Al, Cu, Mg, Si and Zn, it has been verified that the best heat storage densities on a mass or volume basis are obtained with alloys rich in Si or Al, elements that have large heats of fusion. Several of these alloys have the highest heat-storage density reported for phase change materials that transform between 780 and 850 K. The Mg<sub>2</sub>Si-Si eutectic, which has outstanding storage density at 1219 K, illustrates the utility of ordered intermetallic phases with large heat of formation that dissolve in the eutectic liquid to contribute to the entropy change.

PHASE change materials (PCMs) are being explored as heat storage media to reduce the costs of energy generation, conversion and distribution systems. At low temperatures, phase changes in Glauber's salt, Na<sub>2</sub>SO<sub>4</sub> · 10H<sub>2</sub>O, and other salts have been studied for decades as alternatives to heat capacity storage in water or rocks.<sup>1</sup> Rising energy costs and attempts to harvest solar radiation have intensified interest in high temperature storage. The suitability of PCM systems for this purpose has been recognized for years.<sup>2</sup> However, systematic study of alloys instead of inorganic salts has been limited to very rough calculations on pure metals and a few binary alloys.<sup>2,3</sup> This study explores the characteristics that make some alloys better than others. Experimental heat of transformation measurements on promising alloys of the relatively plentiful metals Al, Cu, Mg, Si and Zn provide values for the maximum possible heat storage densities in these alloys.

The heat available from a phase transformation carried out reversibly at constant temperature and pressure is the enthalpy change, which is equal to the transformation temperature multiplied by the entropy change. A sample calculation applied to the fusion of an average close-packed metal illustrates the advantage of a PCM over heat capacity storage.

The entropy of fusion of a normal fcc or hcp metal is shown to be about 10 joules per gram atom per kelvin in Fig. 1.<sup>4</sup> The molar heat capacities are not so uniform, but average about 30 joules per gram atom per kelvin. Fusion of a gram atom of such a metal at 800 K yields 8 kJ, which could be stored in heat capacity only by a temperature rise of 270 K. In practice, the temperature rise is restricted by using much more storage material and a much larger container. In many heat storage systems, the cost of the containing structure and heat exchange surfaces is likely to exceed the cost of storage material, so heat storage density is very important. The advantages of even larger transformation enthalpies that might seem to accrue from the transformation of a

condensed phase to a gas are offset by the large system volumes that are required to handle the gases. Metals and alloys, because of their high thermal conductivities, offer an important advantage in that the ratio of heat exchanger area to storage volume can be much smaller, for a fixed cycling time, than it is for more poorly conducting materials.<sup>2</sup>

Any energy storage system having a large central unit or many smaller units must use cheap, plentiful materials. An analysis<sup>3</sup> of a number of elements indicated that nine elements, S, Al, Si, Zn, P, Na, Cu, Mg, Ca, should be given greatest consideration. Pb addition could also be considered in small amounts, while Sb, Cd, Sn were ruled out for large scale applications.

## THERMODYNAMIC EQUATIONS FOR EUTECTIC MELTING

Using standard procedures of classical thermodynamics and common approximations, equations have been written for three cases of eutectic transformation<sup>5,6</sup> in binary systems defined by the constructions labeled (a), (b), and (c) in Fig. 2. The approximations are:

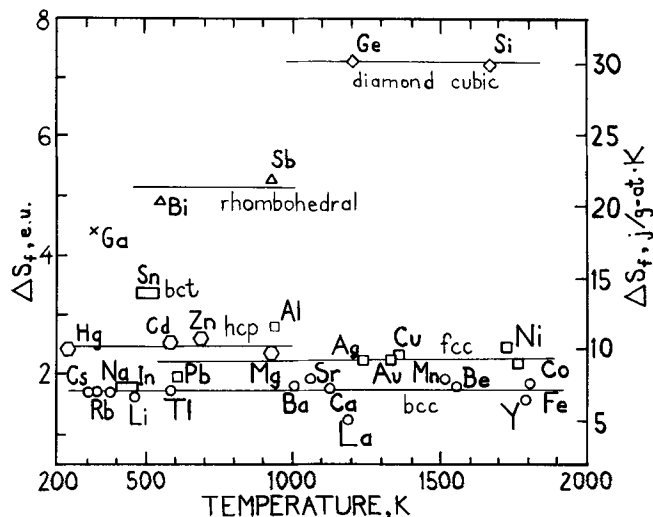


Fig. 1—Entropies of fusion of some elements. Ga is orthorhombic; In is face-centered tetragonal. The figure has been modified from Ref. 4, using data from Ref. 8.

C. ERNEST BIRCHENALL is Distinguished Professor of Metallurgy, Department of Chemical Engineering, University of Delaware, Newark, DE 19711. ALAN F. RIECHMAN is Materials Engineer, E. I. duPont de Nemours and Co., Inc., Beaumont, TX 77704.

Manuscript submitted July 16, 1979.

1) differences between heat capacities of the eutectic liquid and solid can be neglected for a moderate temperature variation near the eutectic temperature  $T_e$ , or the equivalent assumption, the latent heat  $L$ , and the entropy change  $\Delta S = L/T_e$  of the eutectic transformation are independent of temperature near  $T_e$ ; 2) the heat of formation  $\Delta H$  from the pure solid elements of an ordered intermetallic solid phase  $\epsilon$  is equal to the Gibbs free energy of formation  $\Delta G$  because the entropy change must be very small; 3) the entropy change during eutectic melting consists of the entropies of fusion of the pure components plus the entropy for random mixing of these components in the liquid eutectic less the entropies for random mixing in the solid solutions. The last assumption is equivalent to treating all solutions as regular solutions and all intermediate phases as completely ordered. All other terms in the equation for the Gibbs free energy change can be assigned to the enthalpy change, because the Gibbs free energy change for the eutectic reaction at  $T_e$  must be zero.

Using these approximations, the entropy change for case 2 (Fig. 2) is

$$\begin{aligned} \Delta S = -R \left\{ (1 - x_e) \ln(1 - x_e) + x_e \ln x_e \right. \\ \left. - \left( \frac{x_\beta - x_e}{x_\beta - x_\alpha} \right) [(1 - x_\alpha) \ln(1 - x_\alpha) + x_\alpha \ln x_\alpha] \right. \\ \left. - \left( \frac{x_e - x_\alpha}{x_\beta - x_\alpha} \right) [(1 - x_\beta) \ln(1 - x_\beta) \right. \\ \left. + x_\beta \ln x_\beta] \right\} + (1 - x_e) \frac{L_A}{T_A} + x_e \frac{L_B}{T_B} \quad [1] \end{aligned}$$

Extending this procedure to greater numbers of components adds additional terms of the same kind. In this way the entropy change can be increased by mixing more and more components if they are present in nearly equal proportions. Although this work is concerned

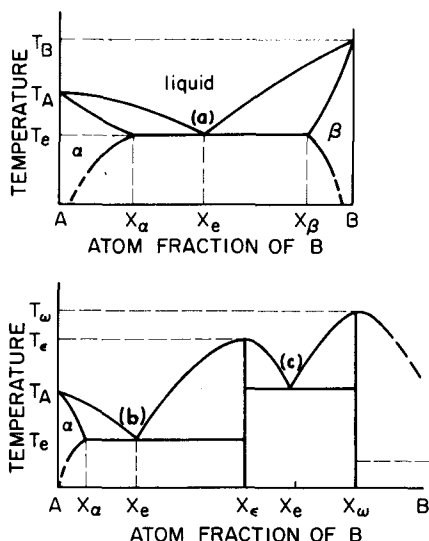


Fig. 2—Eutectic construction for binary systems: (a) Eutectic liquid forms from two solid solutions; (b) Eutectic from one solid solution and one intermetallic phase; (c) Eutectic from two intermetallic phases.

with binary systems and a few ternary systems, it is intended to use this base to seek higher order eutectics that yield the benefits of increased entropy of mixing. The equation also shows that the largest contributions are provided by those elements that have the highest entropies of fusion. Among the inexpensive elements, silicon and aluminum deserve special attention, according to Fig. 1.

With the entropy contributions identified, the enthalpy change at the eutectic temperature can be found in two ways: 1) by multiplying  $\Delta S$  by  $T_e$  and 2) by evaluating the remaining terms in the free energy equation. Comparison of these numbers would be a direct check on the validity of the separation of contributions if the data were sufficiently precise. However, the comparisons also help to identify questionable data. The heat effect given by the remaining terms in the free energy equation is

$$\begin{aligned} \Delta H = (1 - x_e)L_A + x_e L_B + RT \left\{ (1 - x_e) \ln \gamma_A^e \right. \\ \left. + x_e \ln \gamma_B^e - \left( \frac{x_\beta - x_e}{x_\beta - x_\alpha} \right) [(1 - x_\alpha) \ln \gamma_\alpha^e \right. \\ \left. + x_\alpha \ln \gamma_\beta^e] - \left( \frac{x_e - x_\alpha}{x_\beta - x_\alpha} \right) [(1 - x_\beta) \ln \gamma_\beta^e \right. \\ \left. + x_\beta \ln \gamma_\alpha^e] \right\} \quad [2] \end{aligned}$$

where the  $\gamma$ 's are activity coefficients.

At the same composition, the activity coefficients ordinarily differ more strongly from unity for the solid phases than for the liquid phases, a tendency reinforced by the increasing deviation from unity with decreasing temperature. On the other hand, the most desirable liquids are more concentrated solutions than the solid phases that react to form them, so the greater deviations from unity are likely to be displayed by the activity coefficients for the liquids. Unfortunately, the direct experimental measurements of thermodynamic quantities for metallic solutions usually are terminated considerably above the eutectic temperatures, and often are completely unavailable for the solid phases. In those cases, only rough extrapolations and judicious guesses can be used. Clearly, it is desirable to have large latent heats of fusion for all components, combined with narrow ranges of solid solubility, in which there are strong negative deviations from ideal solution behavior, and a eutectic liquid that exhibits much weaker negative deviations.

A second case is found frequently in which a solid solution  $\alpha$  and an intermediate phase  $\epsilon$  combine to form the eutectic, as in Fig. 2 at point b. Neglecting any entropy of mixing in  $\epsilon$ , the appropriate modifications are made readily in Eqs. [1] and [2].

$$\begin{aligned} \Delta S = -R \left\{ (1 - x_e) \ln(1 - x_e) + x_e \ln x_e \right. \\ \left. - \left( \frac{x_e - x_\alpha}{x_e - x_\epsilon} \right) [(1 - x_\alpha) \ln(1 - x_\alpha) + x_\alpha \ln x_\alpha] \right\} \\ + (1 - x_e) \frac{L_A}{T_A} + x_e \frac{L_B}{T_B} \quad [3] \end{aligned}$$

$$\Delta H = RT \left\{ (1 - x_e) \ln \gamma_A^e + x_e \ln \gamma_B^e - \left( \frac{x_e - x_a}{x_e - x_a} \right) [(1 - x_a) \ln \gamma_A^a + x_a \ln \gamma_B^a] \right\} + (1 - x_e) L_A + x_e L_B + \left( \frac{x_e - x_a}{x_e - x_a} \right) \Delta H_\epsilon \quad [4]$$

Note that the activity coefficients for the components in the intermediate phase are replaced by the equivalent heat of formation, which is more likely to be tabulated.

The final case to be considered is that in which two ordered intermediate phases  $\epsilon$  and  $\omega$  combine to form a eutectic melt as illustrated in Fig. 2 at point c. The analogs of Eqs. [1] and [2] now become:

$$\Delta S = -R [(1 - x_e) \ln (1 - x_e) + x_e \ln x_e] + (1 - x_e) \frac{L_A}{T_A} + x_e \frac{L_B}{T_B} \quad [5]$$

$$\Delta H = RT [(1 - x_e) \ln \gamma_A^e + x_e \ln \gamma_B^e] + (1 - x_e) L_A + x_e L_B + \left( \frac{x_\omega - x_e}{x_\omega - x_e} \right) \Delta H_\epsilon + \left( \frac{x_e - x_\epsilon}{x_\omega - x_\epsilon} \right) \Delta H_\omega \quad [6]$$

The last case makes it clear by comparing Eqs. [5] and [6] that the separation of entropy and enthalpy of transformation cannot be exact, because Eq. [5] does not contain any explicit properties of  $\epsilon$  and  $\omega$ . They only need to form with sufficient strength of binding to suppress substitutional disorder. Thus, Eq. [6] seems likely to give a better estimate of the heat storage capabilities of such systems. In the calculations to follow, the values for estimated heat storage based on  $T\Delta S$ , that is on Eqs. [1], [3] and [5], are designated as the first approximation, while the values based on  $\Delta H$ , as given in Eqs. [2], [4] and [6] are designated as second approximations and are given in parentheses in Table I. The latter, however, are more sensitive to experimental errors in the tabulated data, so they are not necessarily more reliable than the first approximations. Our direct measurements can be compared with these calculated values.

### Experimental Procedure

The enthalpy changes for several binary and ternary eutectic alloys were measured by differential scanning calorimetry for temperatures below 1020 K (Perkin-Elmer DSC-2) and by differential thermal analysis for temperatures above 1020 K (Du Pont 900DTA with high temperature cell). The compositions and temperatures of transformation were obtained from published phase diagrams.<sup>8-10</sup> Alloys were melted from commer-

**Table I. Heats of Eutectic Transformation (Maximum Heat Storage Capacity) and Undercooling of Selected Binary and Ternary Metal Eutectics**

Eutectic Alloy, Mol Fractions	Eutectic Temperature, K	Undercooling, K	Compositions <sup>9</sup>		Heat of Formation, <sup>7,9</sup> kJ/g · at.	Maximum Heat Storage, kJ/kg	
			$x_a$	$x_c$		Calculated†	Measured
<b>Binaries</b>							
Mg-0.29 Zn	616	2-4	0.025	0.30*	12.6	247 (464)	138
Al-0.375 Mg	724	5-9	0.19	0.38‡	3.05	458 (477)	310
Al-0.175 Cu	821	1-3	0.025	0.333	13.3	359 (380)	351
Al-0.13 Si	852	2-3				571	515
Mg-0.529 Si	1219	1-2	1.0	0.333	26.4	1212	774
Proportion <sup>10</sup> of Phases							
<b>Ternaries</b>							
Al-0.17 Cu -0.162 Mg	779	4-10	$f_a = 0.354$		$\approx 1.5$	406 (400)	360
			$f_{\text{CuMgAl}_2} = 0.620$		$\begin{cases} 8.0 \\ 13.25 \\ \approx 3.6 \text{ (eutectic)} \end{cases}$		
			$f_{\text{CuAl}_2} = 0.026$				
Al-0.126 Cu -0.051 Mg	833	5-6	$f_{\text{Mg}_2\text{Si}} = 0.067$		26.4	549 (449)	545
			$f_{\text{Si}} = 0.094$				
			$f_a = 0.838$	$\begin{cases} 0.981 \text{ Al} \\ 0.11 \text{ Si} \\ 0.0076 \text{ Mg} \end{cases}$			

\* Values not in parentheses are calculated from Eqs. [1], [3], or [5]. Values in parentheses are calculated from Eqs. [2], [4] or [6].

† Structure of intermediate phase is unknown. Heat of formation estimated to be less than that of  $\text{MgZn}_2$  (17.6 kJ/g · at.). An even smaller  $\Delta H_\epsilon$  or a disordered solid phase would lower the calculated heat storage in parentheses.

‡ Melts congruently at  $\text{Al}_3\text{Mg}_2$  and 724 K.

cially pure elements in graphite crucibles. The eutectic structure, in each case, was verified by optical metallography to be fine enough that a small sample would represent the bulk alloy. Proper behavior of the DSC and DTA curves also verified the absence of any significant excess of either phase.

The measurements were calibrated by runs on six carefully purified elements. Small alloy samples were melted and refrozen in graphite liners to insure good thermal contact prior to the first measurement. The samples were then measured repeatedly to ascertain that the transformation temperatures and heats of transformation were reproducible. For the DSC measurements, good determinations of heat capacity also were made. Only the  $Mg_2Si$ -Si alloys at very high temperature in the DTA apparatus showed a drift in behavior, which was attributed to small losses of the volatile Mg metal. Although this drift was minimized by using crucibles with good closure in inert gas, the values reported are those obtained in the first cycle. Even so, the enthalpy change listed for that alloy may be low.

The alloys selected for measurement are those containing the plentiful elements for which the theory and preliminary calculations based on published data predicted the highest heats of transformation. Other eutectics from these same systems and eutectics from other binary systems did not seem likely to yield maximum storage densities as high as these. Many ternary systems are incompletely known, so other ternary alloys may be measured later from ternary systems that have been examined in part.

Calibration of the DTA apparatus indicated that a precision of  $\pm 4$  pct and  $\pm 3$  K could be expected for the enthalpy of fusion and temperature, respectively. Heat capacity could not be obtained with useful precision. For the DSC apparatus, precision of  $\pm 2$  pct and  $\pm 1$  K could be expected for the enthalpy change and temperature, respectively. Furthermore, heat capacities could be measured to about  $\pm 10$  pct or better. Additional uncertainties can arise if the composition is not precisely at the eutectic value, but a small amount of an excess phase makes a comparable heat contribution of its own, so that the effect should not be a sensitive one.

#### Summary of Calculations and Measurements on Binary and Ternary Eutectic Alloys

Table I summarizes measurements and calculations for the chosen systems. For Mg-Zn and Mg-Si, the measured values lie far below the calculated values. The Al-Mg result also is seriously below predictions. Al-Cu and Al-Si-Mg give very close agreement. Al-Si and Al-Cu-Mg are satisfactorily close to the predicted values. Calculations based on the available, tabulated data are not a satisfactory substitute for measurements on the eutectic alloys.

The undercoolings recorded for all of these alloys are based on the very small samples used in the thermal analysis measurements. The starting materials were commercially pure metals, not research grade materials. However, commercially pure metals usually contain very little impurity to act as nucleation catalysts. The small samples tend to undercool more than larger

amounts of the same alloy. If there is a need to restrict undercooling to less than the 5 to 10 K range observed for several systems, intentionally added dopants and larger samples should eliminate the problem. In any case, a real system is not likely to undercool to the extent reported here.

The heat capacities measured on the DSC for all alloys listed in Table I are given in Table II. Those heat capacities apply to the solid mixture at the transformation temperature. Some of the other heat capacities in Table II taken from previous tabulations may apply at room temperature.

## DISCUSSION

Definitive comparisons among the materials that have been proposed for high temperature storage are premature because the tabulated data may be uncertain, and some critical data are completely missing. Table II contains a preliminary comparison with salts identified by Tye *et al.*,<sup>11</sup> and Kauffman and Lorsch<sup>2</sup> to have merit because of unusually high storage density or a good temperature match to a particular heat generating device. Lithium-containing compounds and fluorides stand out because of their low atomic numbers. The studies of Schröder<sup>12</sup> have emphasized fluoride eutectics, and the Dynatech studies<sup>11</sup> have emphasized lithium compounds and eutectics.

The relatively high cost of these materials, especially of lithium and lithium hydride, must be borne in mind. Also, the salts must be dried very carefully and kept dry to limit their corrosive attack on containers. Volume change measurements on transforming salts and salt eutectics are sparse. However, their volume changes for solid-liquid transformations sometimes are large;<sup>2</sup> for example, values in excess of 20 pct are reported for melting LiF, LiCl, NaF, NaCl, LiNO<sub>3</sub>, and the 63LiOH/37LiCl eutectic.<sup>11</sup> In contrast, the alloy transformations appear to involve changes appreciably less than 10 pct. For the Al-Al<sub>2</sub>Cu eutectic transformation the volume was found to increase by 5.1 pct during fusion by Birchenall, Harrison and Balart.<sup>13</sup>

Where thermal conductivities of salts are given, they lie in the range 1 to 5 W/m · K, except that LiH has a value of 7. The solid metals have thermal conductivities of 40 to 400 W/m · K, and the alloys and liquid metals may drop to about half of these values, retaining an advantage of one to two orders of magnitude.

Tye *et al.*<sup>11</sup> specified important temperature ranges to match the principal heat-generating sources: water-cooled nuclear reactors (PWR and BWR), 505 to 544 K: fossil-fueled supercritical-steam reactor (FFR), 783 to 853 K: high-temperature, gas-cooled, graphite-moderated nuclear reactor (HTGR), 977 to 1033 K. The storage materials studied for these cases were: LiNO<sub>3</sub> (527 K for PWR), 63LiOH/37LiCl eutectic (533 K for BWR), LiOH (743 K for FFR), and Na<sub>2</sub>B<sub>4</sub>O<sub>7</sub> (1015 K for HTGR). However, Na<sub>2</sub>B<sub>4</sub>O<sub>7</sub> usually did not crystallize. Glass-forming borates, silicates and phosphates are unsuitable PCM's for heat storage applications. Thus, lithium salts are the basis of all of the workable materials in that study.

Table II. Comparison of Phase-Change Materials as Heat Storage Media

Material (wt pct)	Transformation Temperature, K	Heat of Transformation, kJ/kg	Solid† Density, kg/m <sup>3</sup>	Volumetric <sup>Δ</sup> Heat Storage, kJ/m <sup>3</sup>	Solid Heat Capacity kJ/kgK	Coefficient of <sup>ε</sup> Thermal Conduction W/mK
Mg <sub>2</sub> Si/Si	1219*	774*	(2000)‡	1.55 × 10 <sup>6</sup>	—	26/20
LiF	1121	1044	2640	2.76	1.64	1.92
75NaF/25MgF	1105	650	2680	1.74	1.42	4.66
67LiF/33MgF <sub>2</sub>	1019	947	2630	2.49	1.42	—
65NaF/23CaF <sub>2</sub> /12MgF <sub>2</sub>	1018	574	2760	1.58	1.17	—
Li <sub>2</sub> CO <sub>3</sub>	998	605	2200	1.33	2.64	—
CaMg <sub>2</sub>	990	554	(1550)‡	0.86	—	4/20
MgCl <sub>2</sub>	988	454	2240	1.02	0.75	—
LiH	956	2582	790	2.04	8.04	7.0
Al	934	400	2370‡	0.95	1.29*	204.2
33.4LiF/49.5NaF/17.1MgF <sub>2</sub>	923	860	2810	2.42	1.42	1.15
Mg	922	368	1590‡	0.59	1.34	131
46LiF/44NaF/10MgF <sub>2</sub>	905	858	2610	2.24	1.40	1.20
MgZn <sub>2</sub>	861	275	5200	1.43	—	—
Al/Si	852*	515*	(2250)*	1.16	1.49*	180/70
Ca(NO <sub>3</sub> ) <sub>2</sub>	834	130	2500	0.33	0.88	—
Al/Si/Mg	833*	545*	(2300)*	1.25	1.39*	200/70
Al/Al <sub>2</sub> Cu	821*	351*	3424‡	1.20	1.11*	130/80
Mg/Mg <sub>2</sub> Ca	790	(353)	(1570)‡	0.55	—	—
Al/Al <sub>2</sub> Cu/Al <sub>2</sub> CuMg	779*	360*	(3050)‡	1.10	1.09*	115/75
56Na <sub>2</sub> CO <sub>3</sub> /44Li <sub>2</sub> CO <sub>3</sub>	769	368	2330	0.86	1.85	2.11
LiOH	744	1100	1340‡	1.47	4.5	1.3
Al/Mg <sub>2</sub> Al <sub>3</sub>	724*	310*	(2300)‡	0.71	1.73*	80/50
50NaCl/50MgCl <sub>2</sub>	723	429	2240	0.96	0.93	0.96
LiOH/LiF	700	1163	1150	1.34	2.14	1.2
Zn	693	112	7140	0.80	0.45	—
31Li <sub>2</sub> CO <sub>3</sub> /35K <sub>2</sub> CO <sub>3</sub> /33Na <sub>2</sub> CO <sub>3</sub>	670	275	2310	0.64	1.69	2.04
63MgCl <sub>2</sub> /22.3NaCl/14KCl	658	461	2250	1.04	0.96	0.95
Mg/Mg <sub>2</sub> Zn	616*	138*	(4900)	0.68	1.04*	80/50
NaOH	593	160	2070	0.33	1.47	1.54
95.4NaNO <sub>3</sub> /4.6NaCl	570	191	2260	0.43	1.85	0.61
7.8NaCl/6.4Na <sub>2</sub> CO <sub>3</sub> /85.8NaOH	555	316	2130	0.67	2.51	—
37LiCl/63 LiOH	535	485	1550	0.75	2.4	1.10
LiNO <sub>3</sub>	527	530	2120	1.12	2.05	1.37
Li	452	663	534	0.35	3.98	—

\* Measured or confirmed in this work.

† Density values in parentheses are estimated from the behavior of the elements. Other values are from tables cited.

‡ Density at transformation temperature; others appear to be at room temperature, which inflates volumetric heat storage density.

Δ These values depend on the densities. Nearly all will be lowered further when based on liquid volume.

ε Where two numbers are given, the first is an estimate for the solid, the second for the liquid, both at transformation temperature.

Other large-scale applications may be possible in these and other temperature ranges. For example, central station solar thermal power generation might be compatible with storage between 600 and 930 K, depending on the type of conversion cycle with which it is coupled. Intermediate scale industrial and transportation applications also may spread over a wide temperature range, including temperatures above 1600 K for steel soaking pits. Small-scale storage applications, at widely scattered temperatures, also take place downstream from the power generator. If those applications are built around a heat-storage system, they can level the load on the generation and distribution systems. For that reason, Table II is not limited to the three ranges emphasized by Tye *et al.*<sup>11</sup> Entries are listed according to transformation temperature. Values enclosed by parentheses are our calculated or estimated values. Those not so enclosed are either measured values, or are taken directly from tables.<sup>2,11</sup> The density values with double daggers are for the solid at the transformation temperature. All other densities appear to be room tem-

perature values, which gives corresponding volumetric heat storage values that are slightly too high. The solid heat capacities, as well as heats of transformation, and transformation temperatures measured by DSC in this investigation are distinguished by asterisks.

## CONCLUSIONS

From Table II, it appears that the Al-Cu, Al-Si, Al-Cu-Mg and Al-Si-Mg eutectics have the best heat storage characteristics in the range to operate with fossil-fueled combustors. The Mg<sub>2</sub>Si-Si eutectic has very good heat storage capacity at 1219 K, where it might find application in a solar power tower. Heat conduction should offer added advantages over other types of materials, especially for short charging or discharging times.<sup>2</sup> In the HTGR and central-station, solar-thermal range, the metallic materials must compete with fluoride mixtures unless the operating temperature is high enough to be compatible with the magnesium-silicon eutectic, or unless that transformation temperature can

be lowered by further alloying. In the intermediate temperature range LiH has outstanding storage capability on a mass basis, but it is very reactive and expensive. Ternary fluoride mixtures appear to be preferable on a volume basis.

A similar sort of comparison might be made between LiOH, one of the least expensive lithium compounds, NaCl-MgCl<sub>2</sub>, and the Al-Mg eutectic, where high thermal conductivity may favor the alloy for some purposes. LiOH/LiF, Li<sub>2</sub>CO<sub>3</sub>/K<sub>2</sub>CO<sub>3</sub>/Na<sub>2</sub>CO<sub>3</sub>, and Zn may offer a similar choice, to be determined by conduction and containment problems that are not definable without specifying an application. If metals are to play any role below the Mg/Mg<sub>2</sub>Zn eutectic temperature, it must be for small-scale special applications that justify the use of relatively expensive metals, or they must wait for ternary or more complex systems that remain to be identified.

#### ACKNOWLEDGMENT

Financial support for this work was provided by the Energy Research and Development Administration through Contract No. E(11-1)-4042. We appreciated thoughtful discussions with the program monitor, Mr. Joseph P. Joyce of the NASA-Lewis Research Center. Professor Robert Rapp, of Ohio State University, also

made valuable suggestions that are reflected in the manuscript.

#### REFERENCES

1. M. Telkes: *ASHRAE J.*, September 1974, pp. 38-44.
2. K. W. Kauffman and H. G. Lorsch: Preprint 76 WA/HT-34, ASME, December 1976. Available on request from the authors, Franklin Institute Research Center, Philadelphia, PA.
3. C. E. Birchenall and M. Telkes: *Sharing the Sun*, K. W. Böer, ed., vol. 8, pp. 138-54, Pergamon Press, NY, 1976.
4. A. P. Miodownik: *Metallurgical Chemistry Symposium*, O. Kubaschewski, ed., pp. 233-44, HMSO (London), 1972.
5. K. Denbigh: *The Principles of Chemical Equilibrium*, 3rd ed., p. 215ff, Cambridge University Press, London, 1971.
6. A. Horsthemke and E. Marschall: *Brennstoff-Warme-Kraft*, 1976, vol. 28, p. 18.
7. O. Kubaschewski, E. L. Evans, and C. B. Alcock: *Metallurgical Thermochemistry*, 4th ed., p. 210ff, Pergamon Press, NY, 1967.
8. R. Hultgren, P. D. Desai, D. T. Hawkins, M. Gleiser, and K. K. Wagman: *Selected Values of the Thermodynamic Properties of the Elements*, ASM, Metals Park, OH, 1973.
9. R. Hultgren, P. D. Desai, D. T. Hawkins, M. Gleiser, and K. K. Kelley: *Selected Values of the Thermodynamic Properties of Binary Alloys*, ASM, Metals Park, OH, 1973.
10. *Metals Handbook*, 4th ed., vol. 8, ASM, Metals Park, OH, 1974.
11. R. P. Tye, J. G. Bourne, and A. O. Desjarlais: NASA Report No. NASA-CR-135098, August 1976 (Dynatech Corp.), available from NTIS.
12. J. Schröder: *J. Eng. Ind.*, 1975, vol. 97, pp. 893-96.
13. C. E. Birchenall, A. J. Harrison, and S. N. Balart: *Met. Trans. A.*, 1980, vol. 11A, p. 1213.